RSC Advances

PAPER

View Article Online
View Journal | View Issue

Cite this: *RSC Adv.*, 2025, **15**, 8777

Synthesis of nanoscale surfactant-encapsulated silica-supported polyoxometalate [Si/AlO_2]@[PWZn]@CTAB and its catalytic application in the oxidation of alcohols†

Mohammad Alizadeh and Bahram Yadollahi *

Received 4th February 2025
Accepted 17th March 2025

DOI: 10.1039/d5ra00821b

rsc.li/rsc-advances

Silica-supported polyoxometalates [Si/AlO_2]@[PWM] (M = Zn, Cu, Ni, Co, Fe, Mn, and Cr) were produced by immobilizing transition metal substituted Keggin-type polyoxometalates on cationic silica nanoparticles. These silica-supported polyoxometalates were then encapsulated with hexadecyltrimethylammonium bromide to obtain [Si/AlO_2]@[PWM]@CTAB (M = Zn, Cu, Ni, Co, Fe, Mn, and Cr) to prevent polyoxometalate leaching. Characterization by FT-IR, TG-DTG, XRD, SEM, and TEM indicated that the polyoxometalate structure was retained after immobilization and encapsulation. These nanoscale compounds were used as heterogeneous catalysts in the oxidation of various alcohols, achieving very good to excellent yields with H_2O_2 as an oxidant, and demonstrating high reusability. These benefits introduce surfactant-encapsulated silica-supported polyoxometalates as highly efficient heterogeneous catalysts in different oxidation reactions.

Introduction

Polyoxometalates (POMs) as oxygen-containing inorganic cluster systems are known for their excellent properties in various fields, including catalysis,[1–3] hybrid materials,[4–6] and medicines.[7–10] The special physicochemical properties, thermal stability, solubility, structure, topology, and electronic behaviour of POMs are crucial for their catalytic applications.[11,12] Because of strong acidity and rich redox properties, various POMs have been used as catalysts in different chemical syntheses.[13–16] One of the most investigated methods using POM catalysts is the catalytic oxidation of organic compounds.

Transition metal substituted Keggin-type POMs with the general formula $[XW_{11}M(L)O_{39}]^{m-}$ (X = P, Si, M = transition metal, and L = H_2O or other monodentate ligands) have garnered significant interest due to their potential to control chemical properties *via* transition metal substitution.[17–19]

One of the most important functional group transformations in modern organic synthesis is the selective oxidation of alcohols into the corresponding aldehydes and ketones. Traditional methodologies use stoichiometric heavy metal reagents (*e.g.*, Cr, Mn) in this oxidation reaction.[20] As better alternatives, catalytic oxidations with *tert*-butyl hydroperoxide, hydrogen peroxide, oxygen, and other oxidants have also been developed.[21–28] Hydrogen peroxide, frequently used due to its higher active oxygen content and water as the only by-product, is particularly effective for alcohol oxidation when combined with POMs.[28–40] For instance, $Na_{12}[WZn_3(H_2O)_2][ZnW_9O_{34}]_2$, $Na_9[SbW_9O_{33}]$, $Na_4H_3[SiW_9Al_3(H_2O)_3O_{37}]$, $[n\text{-}C_{16}H_{33}N(CH_3)_3]_3\text{-}PW_{12}O_{40}$, and $[WZnMn_2(H_2O)_2(ZnW_9O_{34})_2]^{12-}$ have been employed for the oxidation of various alcohols with H_2O_2 as the oxidant.[32,41–44]

Due to the low surface area and solubility of POMs in polar reaction systems, their separation and use as heterogeneous catalysts pose some challenges.[45,46] Hence, the immobilization of POMs on solid supports such as silica and silica–alumina, activated carbon and carbon nanotubes, MCM-41, zeolite, chitosan, polymers, and core–shell-type POM composites has been extensively studied.[47–61] However, the continuous leaching of POM into the reaction medium remains a significant problem for supported POM catalysts in polar reaction systems.[62–64]

In this work, we synthesized and immobilized some first-row transition metal substituted Keggin-type POMs such as $[PW_{11}CrO_{39}]^{4-}$, $[PW_{11}MnO_{39}]^{5-}$, $[PW_{11}FeO_{39}]^{4-}$, $[PW_{11}CoO_{39}]^{5-}$, $[PW_{11}NiO_{39}]^{5-}$, $[PW_{11}CuO_{39}]^{5-}$, and $[PW_{11}ZnO_{39}]^{5-}$ on cationic silica nanoparticles with high surface area. To prevent catalyst leaching, the silica-supported POMs were encapsulated with cetyltrimethylammonium bromide (CTAB) (Scheme 1). The catalytic activity of these surfactant-encapsulated silica-supported POMs (SSPOMs) in the oxidation of various alcohols was then investigated.

Department of Chemistry, University of Isfahan, Isfahan 81746-73441, Iran. E-mail: yadollahi@chem.ui.ac.ir

† Electronic supplementary information (ESI) available. See DOI: https://doi.org/10.1039/d5ra00821b

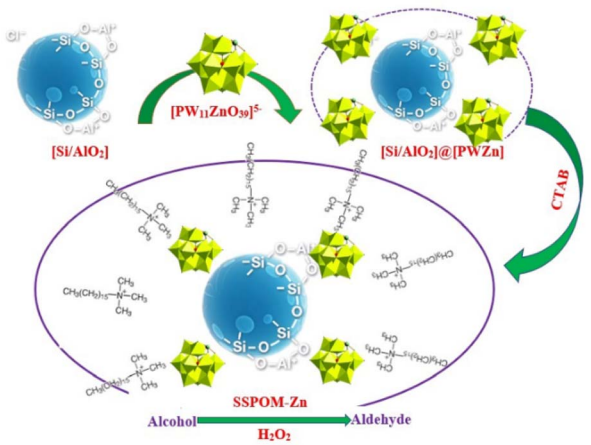

Scheme 1 Schematic representation of the synthesis and catalytic application of SSPOM-Zn in alcohol oxidation.

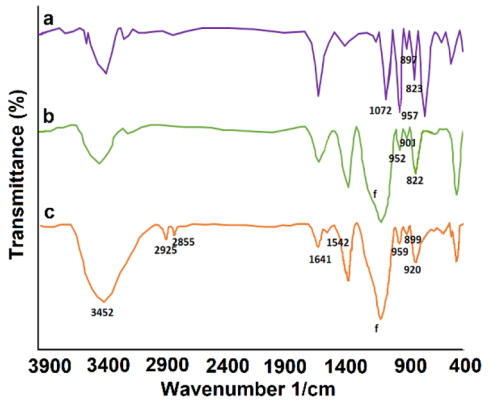

Fig. 1 The FT-IR spectra of $[PW_{11}Zn(H_2O)O_{39}]^{5-}$ (a), $[Si/AlO_2]$@[PWZn] (b), and SSPOM-Zn (c).

Experimental

Materials, instruments, and synthetic methods

All reagents and raw materials were purchased from reputable chemical companies and used without further purification. Bindzil CAT 80 colloidal silica ($[Si/AlO_2]Cl$) with particular specifications (surface area: 85 $m^2\ g^{-1}$, particle size: 40 nm, SiO_2: 40%, pH: 3–5, positive surface charge, bulk density: 1050–1400 $kg\ m^{-3}$) was purchased from Akzo Nobel. All products were identified by comparing their physical and spectral data with those of authentic samples, and yields refer to gas chromatography (GC) yields.

Thermogravimetric (TG-DTG) analysis was performed on a TG-50 thermogravimetric analyzer from 25–800 °C with a temperature rate of 10 °C min^{-1}. Fourier transform infrared spectra (FT-IR) were obtained from 400–4000 cm^{-1} on a PerkinElmer spectrophotometer (Spectrum 65) using KBr pellets. GC experiments were performed on a Varian CP-3800 gas chromatograph using CP-Wax 52 CB (30 m, 0.25 mm ID, df 0.25 μm) and CP-Sil 8 CB capillary column (30 m, 0.32 mm ID, df 0.25 μm). Scanning electron microscopy (SEM) images of the catalyst were taken on SEM Philips XL 30. Transmission electron microscopy (TEM) images were obtained with a Hitachi H8100 electron microscope with an accelerating voltage of 200 kV without staining. X-ray powder diffraction (XRD) data were obtained on a D8 Advance Bruker using Cu Kα radiation ($\lambda = 1.54$ Å).

Preparation of $[Si/AlO_2]$@[PWZn]

The transition metal substituted POMs, $[PW_{11}M(H_2O)O_{39}]^{(7-m)-}.nH_2O$ (M^{m+} = Cr^{3+}, Fe^{3+}, Mn^{2+}, Co^{2+}, Ni^{2+}, Cu^{2+}, and Zn^{2+}), were prepared according to the literature.[65] For example, an aqueous solution of $[PW_{11}ZnO_{39}]^{5-}$ was prepared by mixing Na_2HPO_4 (9.1 mmol) and $Na_2WO_4 \cdot 2H_2O$ (100 mmol) in water (200 mL), adjusting the pH to 4.8, and then adding the nitrate salt of Zn^{2+} (12 mmol). The aqueous colloidal suspension of Bindzil CAT 80 (100 g) was placed in an ultrasonic bath for 10 min to break up aggregates and then added dropwise to the solution of $[PW_{11}ZnO_{39}]^{5-}$ at 80 °C. The mixture was stirred for 3 h at 25 °C, and the resulting solid was filtered and washed several times with 10 mL portions of acetonitrile. Drying at 120 °C for 2 h gave the product. Infrared spectra of $[Si/AlO_2]$@[PWZn] (cm^{-1}): (P–O), overlapped with silica vibration frequencies; (W–O_d), 952; (W–O_b–W), 901; (W–O_c–W), 822 (Fig. 1b and Table 1). Infrared spectra (cm^{-1}) of $K_5[PW_{11}Zn(H_2O)O_{39}]$: (P–O), 1072; (W–$O_d$), 957; (W–$O_b$–W), 897; (W–$O_c$–W), 823 (Fig. 1a and Table 1).

Synthesis of $[Si/AlO_2]$@[PWZn]@CTAB (SSPOM-Zn)

$[Si/AlO_2]$@[PWZn] (200 mg) was stirred in a solution of CTAB (100 mg) and chloroform (10 mL) for 3 h. The product was filtered and washed several times with 5 mL portions of chloroform. Drying at 120 °C for 2 h yielded SSPOM-Zn. Infrared spectra (cm^{-1}): (P–O), overlapped with silica vibration frequencies; (W–O_d), 959; (W–O_b–W), 899; (W–O_c–W), 820 (Fig. 1c and Table 1).

Typical procedure for oxidation of alcohols

In a typical catalytic oxidation reaction, benzyl alcohol (1 mmol), H_2O_2 (30%; 1 mL), and acetonitrile (3 mL) in the presence of SSPOM-Zn (150 mg) as a catalyst was stirred at reflux in a 25 mL round bottom flask equipped with a reflux condenser. Progress of the reaction was monitored by GC. After completion of the reaction, the catalyst was self-precipitated, and $NaHCO_3$ (10%; 10 mL) was added to the separated liquid phase. The organic phase was extracted with chloroform and dried over

Table 1 Vibrational frequencies (cm^{-1})[a] of $[PW_{11}Zn(H_2O)O_{39}]^{5-}$, $[Si/AlO_2]$@[PWZn], and SSPOM-Zn

Compounds	P–O_a	W=O_d	W–O_b–W	W–O_c–W
$[PW_{11}Zn(H_2O)O_{39}]^{5-}$	1072	957	897	823
$[Si/AlO_2]$@[PWZn]	—[b]	952	901	822
SSPOM-Zn	—[b]	959	899	820

[a] O_a: oxygen bonded to phosphorus atom; O_b: octahedral edge-sharing oxygen; O_c: octahedral corner-sharing oxygen; O_d: terminal oxygen. [b] Overlapped with silica vibrational frequencies.

anhydrous $CaCl_2$. The pure product was obtained after flash chromatography on a short silica gel column with a 3 : 7 ethyl acetate : *n*-hexane eluent.

To study catalyst reusability, the catalyst was filtered out after each reaction run, washed several times with acetonitrile, and dried at 120 °C for 3 h. This catalyst was used for the next run following the above procedure.

Results and discussion

Characterization of [Si/AlO_2]@[PWZn]@CTAB (SSPOM-Zn)

The synthesized hybrid POMs were characterized using FT-IR, XRD, SEM, TEM, and TG-DTG techniques. Table 1 and Fig. 1a–c show the FT-IR data and spectra of $[PW_{11}Zn(H_2O)O_{39}]^{5-}$, [Si/$AlO_2$]@[PWZn], and SSPOM-Zn in the range of 400–4000 cm^{-1}. The FT-IR spectra of Bindzil CAT 80 and CTAB are also shown in Fig. S1a and b.†

The vibration frequency of P–O stretching is observed at 1072 cm^{-1} in the POM FT-IR spectrum (Fig. 1a). Additionally, a strong absorption band at 1125 cm^{-1} is assigned to Si–O stretching in the silica FT-IR spectrum (Fig. S1a†). The overlapping of these two bands can be seen in the SSPOM-Zn spectrum (Fig. 1c). Moreover, the bands at 957, 897, and 823 cm^{-1}, which belong to W=O_d, W–O_b–W and W–O_c–W vibrations in $[PW_{11}Zn(H_2O)O_{39}]^{5-}$ (Fig. 1a), are observed at 959, 899, and 820 cm^{-1} in the SSPOM-Zn spectrum (Fig. 1c). This indicates that the POM structure is retained after supporting on the cationic silica and further encapsulation. The FT-IR spectrum of SSPOM-Zn (Fig. 1c) also shows absorption bands at 3452 and 1641 cm^{-1}, assigned to OH stretching. In the FT-IR spectra of CTAB (Fig. S1b†), two bands at 2850 and 2918 cm^{-1} represent the CH_2 antisymmetric and symmetric stretching modes of the CTAB alkyl chain. Additionally, the CTAB FT-IR spectrum shows a band at 1493 cm^{-1}, attributed to the C–H scissoring vibrations of the CH_3–N^+ moiety. These bands shifted to 2858, 2925, and 1542 cm^{-1} in the FT-IR spectrum of SSPOM-Zn (Fig. 1c), likely due to ionic interactions between POM and CTAB.[66–68]

The powder X-ray diffraction patterns of SSPOM-Zn, [Si/AlO_2]@[PWZn], and Bindzil CAT 80 are shown in Fig. 2a–c. The characteristic peaks of SSPOM-Zn and [Si/AlO_2]@[PWZn] (Fig. 2a and b), which are also present in the XRD pattern of $[PW_{11}Zn(H_2O)O_{39}]^{5-}$,[69] indicate that the POM structure is retained after immobilization and encapsulation.

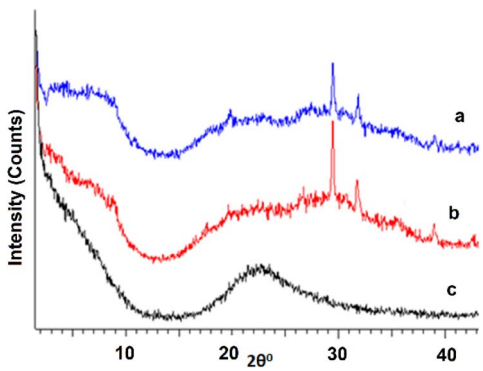

Fig. 2 The XRD pattern of SSPOM-Zn (a), [Si/AlO_2]@[PWZn] (b), and Bindzil CAT 80 (c).

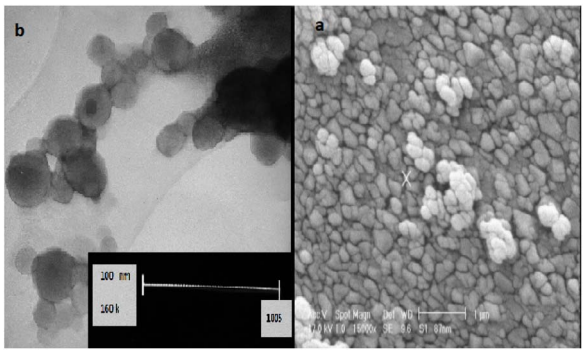

Fig. 3 SEM (a) and TEM (b) images of SSPOM-Zn.

In addition to the XRD pattern, the results of thermogravimetric studies confirmed the formation of SESSP-1. In the silica (Bindzil CAT 80) TG-DTG curve (Fig. S2†), the weight loss at temperatures below 400 °C corresponds to the water abstraction from silica. The TG-DTG profile for [Si/AlO_2]@[PWZn] (Fig. S3†) also shows a weight loss at temperatures below 400 °C, corresponding to the water abstraction from silica and POM. Another weight loss at temperatures above 400 °C is due to the decomposition of the POM structure. Similarly, the TG-DTG diagram for SESSP-1 (Fig. S4†) shows comparable weight losses. As seen in Fig. S4,† the weight loss at about 380 °C can be attributed to the decomposition of surfactant-containing structures, confirming the presence of POM and surfactant on the silica surface.

SEM and TEM images were also used to gather detailed information about the catalyst's surface morphology and particle size. From the SEM and TEM images of SSPOM-Zn (Fig. 3), the SSPOM-Zn morphology consists of spherical-like

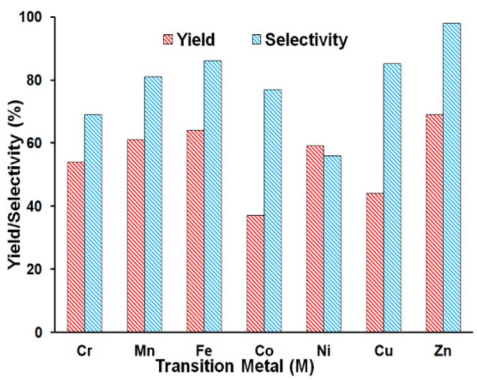

Fig. 4 Oxidation of benzyl alcohol with H_2O_2 in the presence of [Si/AlO_2]@[PWM]@CTAB (SSPOMs; M = Zn, Cu, Ni, Co, Fe, Mn, and Cr) catalysts (reaction conditions: 1 mmol benzyl alcohol, 1 mL H_2O_2, 3 mL CH_3CN, 150 mg catalyst, 5 h reflux; yields refer to GC yields and selectivity is based on the aldehyde).

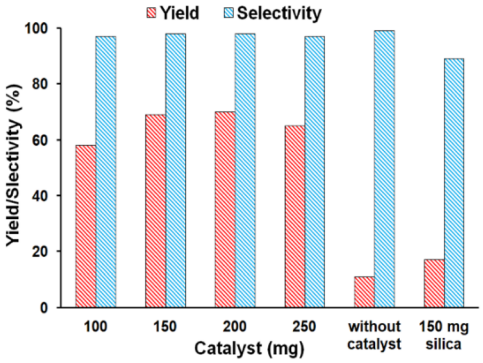

Fig. 5 The effect of SSPOM-Zn amount in the oxidation of benzyl alcohol with H_2O_2 (reaction conditions: 1 mmol benzyl alcohol, 3 mL CH_3CN, catalyst, 1 mL H_2O_2, 5 h reflux; yields refer to GC yields and selectivity is based on the aldehyde).

nanoparticles. Moreover, the average nanoparticle diameter is estimated to be from 20 to 60 nm.

The catalytic activity of [Si/AlO_2]@[PWZn]@CTAB (SSPOM-Zn)

After the preparation and characterization of SSPOMs, their catalytic activities were investigated in the oxidation of alcohols with H_2O_2 as a green oxidant. Benzyl alcohol was chosen as the model substrate, and the reaction conditions were optimized for variables such as the type and amount of catalyst, the amount of oxidant, and the type of solvent. Initially, the oxidation of benzyl alcohol with H_2O_2 in the presence of [Si/AlO_2]@[PWM]@CTAB (SSPOMs; M = Zn, Cu, Ni, Co, Fe, Mn, and Cr) catalysts in acetonitrile was studied. The results (Fig. 4) showed that the Zn-substituted catalyst (SSPOM-Zn) had the highest efficiency in the oxidation of benzyl alcohol among the different transition metal substituted catalysts.

In another investigation, the optimal amount of SSPOM-Zn (0.066 mmole POM on 1 g silica) for the oxidation of benzyl alcohol was determined. Various amounts (0, 100, 150, 200, and 250 mg) of SSPOM-Zn were used, and the results (Fig. 5) indicated that the best yield and selectivity were achieved with 150 mg of SSPOM-Zn. Additionally, the presence of SSPOM-Zn was crucial, as exceptional yields could not be achieved without the catalyst. The oxidation reaction in the presence of cationic silica (used as a blank) did not show notable yields, confirming the catalyst role of Zn-substituted Keggin-type POM in this system.

After optimization of the catalyst amount, the effect of various hydrogen peroxide (30%) values (0.5 to 1.4 mL) was investigated. The results (Fig. 6) showed that the yield and selectivity of benzaldehyde improved with an increase in the amount of oxidant. However, with more than 1 mL of H_2O_2 (up to 1.4 mL), the selectivity of the reaction decreased, leading to a higher production of carboxylic acid.

The effect of various solvents such as CH_3CN, THF, $CHCl_3$, *n*-C_6H_{12}, and $(CH_3)_2CO$, in the oxidation of benzyl alcohol with H_2O_2 was also studied. From the results summarized in Fig. 7, acetonitrile was selected as the best solvent for this reaction.

The efficiency of this method was demonstrated by the successful conversion of various alcohols into the corresponding aldehydes and ketones under the mentioned conditions (Table 2). As seen in Table 2, both benzylic and aliphatic alcohols were converted into the corresponding carbonyl compounds in high to excellent yields.

The conversion of electron-rich benzylic alcohols is faster and more efficient (Table 2, entries 1–4) than electron-deficient benzylic alcohols (Table 2, entries 9 and 10). Cyclic alcohols such as cyclohexanol, cycloheptanol, and 4-methyl cyclohexanol are also converted into the corresponding ketones under these reaction conditions (Table 2, entries 12–14). However, 1-octanol and 1-heptanol did not yield the corresponding aldehyde in good quantities by this method.

In another study, the reusability of SSPOM-Zn was investigated. After filtering, washing, and drying the catalyst at the end of the reaction, it was subjected to another run. According to the results in Fig. 8, the small observed decrease in catalyst activity after five recycling runs, could make it a candidate for further investigation for industrial applications. Moreover, these results suggested no appreciable leaching of the POM from cationic silica nanoparticles during the catalytic reaction.

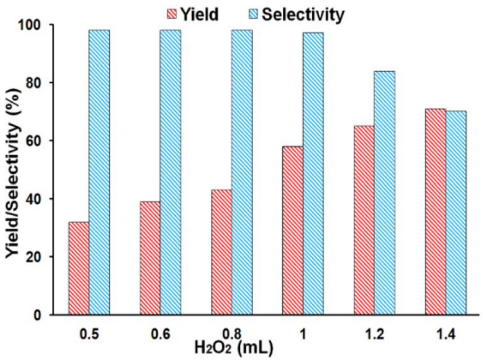

Fig. 6 The effect of H_2O_2 amount in the oxidation of benzyl alcohol (reaction conditions: 1 mmol benzyl alcohol, 3 mL CH_3CN, 100 mg catalyst, 5 h reflux; yields refer to GC yields and selectivity is based on the aldehyde).

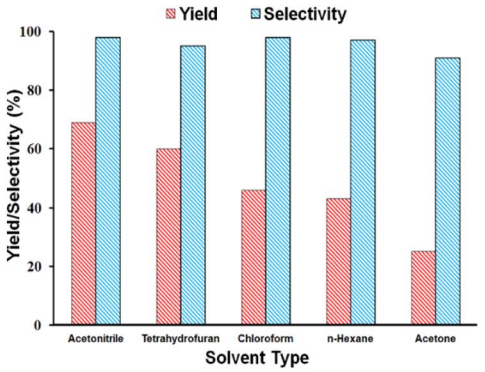

Fig. 7 The effect of solvent type in the oxidation of benzyl alcohol with H_2O_2 (reaction conditions: 1 mmol benzyl alcohol, 1 mL H_2O_2, 150 mg catalyst, 5 h reflux, and 3 mL solvent; yields refer to GC yields and selectivity is based on the aldehyde).

Table 2 Oxidation of various alcohols with H_2O_2 in the presence of SSPOM-Zn as catalyst[a]

Entry	Substrate	Time (h)	Conv.[b] (%)	Selectivity[c] (%)
1	Benzyl alcohol	9	86	95
2	4-Methoxybenzyl alcohol	10	94	96
3	3-Methoxybenzyl alcohol	10	93	93
4	2-Methylbenzyl alcohol	10	91	94
5	2-Bromobenzyl alcohol	15	62	90
6	4-Chlorobenzyl alcohol	15	63	94
7	2-Chlorobenzyl alcohol	15	58	88
8	2,4-Dichlorobenzyl alcohol	15	34	89
9	2-Nitrobenzyl alcohol	15	19	96
10	4-Nitrobenzyl alcohol	15	22	91
11	3,4-Methylenedioxybenzyl alcohol	15	43	80
12	Cyclohexanol	10	82	100
13	4-Methylcyclohexanol	10	87	100
14	Cycloheptanol	10	87	100
15	Butanol	10	3	95
16	Octanol	10	7	96
17	2-Phenyl-1-propanol	10	8	87
18	3-Phenyl-1-propanol	10	6	86

[a] Reaction conditions: 1 mmol alcohol,1 mL H_2O_2, 3 mL CH_3CN, and 150 mg SSPOM-Zn. [b] Conversion refers to GC yields. [c] Selectivity is based on the aldehyde or ketone.

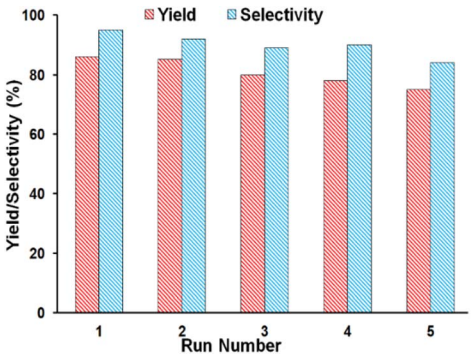

Fig. 8 The reusability of SSPOM-Zn in the oxidation of benzyl alcohol with H_2O_2 (reaction conditions: 1 mmol benzyl alcohol, 1 mL H_2O_2, 150 mg catalyst, 9 h reflux, and 3 mL CH_3CN; yields refer to GC yields and selectivity is based on the aldehyde).

Conclusions

In this work, the successful preparation of transition metal substituted Keggin-type POMs supported on cationic silica and encapsulated by hexadecyltrimethylammonium ions (SSPOMs) was achieved. The prepared catalysts were characterized by FT-IR, XRD, TG-DTG, SEM, and TEM techniques. The results indicated that the POM structure is retained after supporting on the cationic silica and further encapsulation. The average particle diameter of spherical-like nanoparticles containing the SSPOM-Zn was estimated to range from 20 nm to 60 nm. This nanosized catalyst showed efficient activity in the oxidation of alcohols with 30% H_2O_2 in acetonitrile as the solvent. Various alcohols were oxidized to the desired products with high selectivity and very good to excellent yields. The SSPOM-Zn catalyst was easily recycled and used in subsequent catalytic runs. No significant decrease in the catalyst activity was observed after five recycled runs. Therefore, owing to its efficiency, simplicity, cleanliness, cost-effectiveness, reusability, and nanosized characteristics, this system could be a valuable catalytic system for the oxidation of alcohols.

Data availability

The raw/processed data are available in the paper and ESI.†

Author contributions

The study conception and design, material preparation, data collection and analysis were performed by Mohammad Alizadeh and Bahram Yadollahi. The first draft of the manuscript was written by Mohammad Alizadeh and Bahram Yadollahi and all authors read and approved the final manuscript.

Conflicts of interest

There are no conflicts to declare.

Acknowledgements

The authors are grateful to the University of Isfahan for the financial support of this work.

Notes and references

1 Y. Cao, Q. Chen, C. Shen and L. He, *Molecules*, 2019, **24**, 2069.
2 S.-S. Wang and G.-Y. Yang, *Chem. Rev.*, 2015, **115**, 4893.
3 H. Aliyan, R. Fazaeli, N. Fazaeli, A. R. Mssah, H. J. Naghash, M. Alizadeh and G. Emami, *Heteroat. Chem.*, 2009, **20**, 202.
4 J.-Z. Liao, C. Wu, X.-Y. Wu, S.-Q. Deng and C.-Z. Lu, *Chem. Commun.*, 2016, **52**, 7394.

5 M. Alizadeh, B. Yadollahi and A. A. Kajani, *Polyhedron*, 2021, **210**, 115510.
6 Y. Gao, Z. Lv, R. Gao, G. Zhang, Y. Zheng and J. Zhao, *J. Hazard. Mater.*, 2018, **359**, 258.
7 S. Shigeta, S. Mori, T. Yamase, N. Yamamoto and N. Yamamoto, *Biomed. Pharmacother.*, 2006, **60**, 211.
8 L. Zong, H. Wu, H. Lin and Y. Chen, *Nano Res.*, 2018, **11**, 4149.
9 M. B. Čolović, M. Lacković, J. Lalatović, A. S. Mougharbel, U. Kortz and D. Z. Krstić, *Curr. Med. Chem.*, 2020, **27**, 362.
10 M. Alizadeh and B. Yadollahi, *New J. Chem.*, 2022, **46**, 18199.
11 E. Coronado and C. J. Gómez-García, *Chem. Rev.*, 1998, **98**, 273.
12 C. Ritchie, C. Streb, J. Thiel, S. G. Mitchell, H. N. Miras, D. L. Long, T. Boyd, R. D. Peacock, T. McGlone and L. Cronin, *Angew. Chem., Int. Ed.*, 2008, **47**, 6881.
13 M. T. Pope and A. Müller, *Polyoxometalate Chemistry from Topology via Self-Assembly to Applications*, Springer, 2001.
14 J. J. Borrás-Almenar, E. Coronado, A. Müller and M. T. Pope, *Polyoxometalate Molecular Science*, Springer Science & Business Media, 2003.
15 P. Jin, H. Wei, L. Zhou, D. Wei, Y. Wen, B. Zhao, X. Wang and B. Li, *Mol. Catal.*, 2021, **510**, 111705.
16 K. V. Avramidou, F. Zaccheria, S. A. Karakoulia, K. S. Triantafyllidis and N. Ravasio, *Mol. Catal.*, 2017, **439**, 60.
17 F. Cavani, R. Mezzogori, A. Pigamo, F. Trifirò and E. Etienne, *Catal. Today*, 2001, **71**, 97.
18 Z. Zhang, S. Ishikawa, Q. Zhu, T. Murayama, M. Sadakane, M. Hara and W. Ueda, *Inorg. Chem.*, 2019, **58**, 6283.
19 J. Hu, J. Dong, X. Huang, Y. Chi, Z. Lin, J. Li, S. Yang, H. Ma and C. Hu, *Dalton Trans.*, 2017, **46**, 8245.
20 A. Citterio, R. Sebastiano, A. Maronati, F. Viola and A. Farina, *Tetrahedron*, 1996, **52**, 13227.
21 D. Wang, E. W. Qian, H. Amano, K. Okata, A. Ishihara and T. Kabe, *Appl. Catal., A*, 2003, **253**, 91.
22 M. Nakanishi and C. Bolm, *Adv. Synth. Catal.*, 2007, **349**, 861.
23 G. Rothenberg, L. Feldberg, H. Wiener and Y. Sasson, *J. Chem. Soc., Perkin Trans.*, 1998, **2**, 2429.
24 M. J. Ndolomingo and R. Meijboom, *Appl. Surf. Sci.*, 2017, **398**, 19.
25 A. Wusiman and C. D. Lu, *Appl. Organomet. Chem.*, 2015, **29**, 254.
26 R. A. Sheldon, I. W. Arends and A. Dijksman, *Catal. Today*, 2000, **57**, 157.
27 R. A. Sheldon, I. W. Arends, G.-J. Ten Brink and A. Dijksman, *Acc. Chem. Res.*, 2002, **35**, 774.
28 C. M. Crombie, R. J. Lewis, R. L. Taylor, D. J. Morgan, T. E. Davies, A. Folli, D. M. Murphy, J. K. Edwards, J. Qi and H. Jiang, *ACS Catal.*, 2021, **11**, 2701.
29 J. Muzart and A. N. A. Ajjou, *J. Mol. Catal.*, 1991, **66**, 155.
30 D. Lenoir, *Angew. Chem., Int. Ed.*, 2006, **45**, 3206.
31 D. Mansuy, *Pure Appl. Chem.*, 1990, **62**, 741.
32 R. Neumann and M. Gara, *J. Am. Chem. Soc.*, 1995, **117**, 5066.
33 D. Sloboda-Rozner, P. L. Alsters and R. Neumann, *J. Am. Chem. Soc.*, 2003, **125**, 5280.
34 J. Wang, L. Yan, G. Li, X. Wang, Y. Ding and J. Suo, *Tetrahedron Lett.*, 2005, **46**, 7023.
35 M. R. Farsani, E. Assady, F. Jalilian, B. Yadollahi and H. A. Rudbari, *J. Iran. Chem. Soc.*, 2015, **12**, 1207.
36 A. K. Babahydari, R. Fareghi-Alamdari, S. M. Hafshejani, H. A. Rudbari and M. R. Farsani, *J. Iran. Chem. Soc.*, 2016, **13**, 1463.
37 E. Assady, B. Yadollahi, M. Riahi Farsani and M. Moghadam, *Appl. Organomet. Chem.*, 2015, **29**, 561.
38 E. Nikbakht, B. Yadollahi and M. R. Farsani, *Inorg. Chem. Commun.*, 2015, **55**, 135.
39 M. V. Vasylyev and R. Neumann, *J. Am. Chem. Soc.*, 2004, **126**, 884.
40 M. J. da Silva, J. A. V. Torres and C. B. Vilanculo, *RSC Adv.*, 2022, **12**, 11796.
41 D. Sloboda-Rozner, P. Witte, P. L. Alsters and R. Neumann, *Adv. Synth. Catal.*, 2004, **346**, 339.
42 R. H. Ingle, N. K. Raj and P. Manikandan, *J. Mol. Catal. A: Chem.*, 2007, **262**, 52.
43 J. Wang, L. Yan, G. Qian, S. Li, K. Yang, H. Liu and X. Wang, *Tetrahedron*, 2007, **63**, 1826.
44 S. Zhang, G. Zhao, S. Gao, Z. Xi and J. Xu, *J. Mol. Catal. A: Chem.*, 2008, **289**, 22.
45 I. Kozhevnikov, K. Kloetstra, A. Sinnema, H. Zandbergen and H. V. van Bekkum, *J. Mol. Catal. A: Chem.*, 1996, **114**, 287.
46 S. Mukai, L. Lin, T. Masuda and K. Hashimoto, *Chem. Eng. Sci.*, 2001, **56**, 799.
47 M. Sopa, A. Wącław-Held, M. Grossy, J. Pijanka and K. Nowińska, *Appl. Catal., A*, 2005, **285**, 119.
48 M. E. Chimienti, L. R. Pizzio, C. V. Cáceres and M. N. Blanco, *Appl. Catal., A*, 2001, **208**, 7.
49 V. Y. Evtushok, V. A. Lopatkin, O. Y. Podyacheva and O. A. Kholdeeva, *Catalysts*, 2022, **12**, 472.
50 M. Jia, M. Cai, X. Wang, Y. Fang, W. Cao, Y. Song, L. Yuan, Y. Chen and L. Dai, *Mol. Catal.*, 2022, **518**, 112067.
51 G. Karthikeyan and A. Pandurangan, *J. Mol. Catal. A: Chem.*, 2009, **311**, 36.
52 F. Lefebvre, *Inorganics*, 2016, **4**, 13.
53 R. R. Ozer and J. L. Ferry, *J. Phys. Chem. B*, 2002, **106**, 4336.
54 J. H. Advani, B. D. Bankar, H. C. Bajaj and A. V. Biradar, *Cellulose*, 2020, **27**, 8769.
55 X. Lang, Z. Li and C. Xia, *Synth. Commun.*, 2008, **38**, 1610.
56 M. A. Rezvani, M. Shaterian and M. Aghmasheh, *Environ. Technol.*, 2020, **41**, 1219.
57 H. Taghiyar and B. Yadollahi, *Sci. Total Environ.*, 2020, **708**, 134860.
58 L. Rana, *Appl. Catal., A*, 2023, **661**, 119227.
59 O. Makrygenni, D. Brouri, A. Proust, F. Launay and R. Villanneau, *Microporous Mesoporous Mater.*, 2019, **278**, 314–321.
60 C. Jalkh, C. Ghazaly and H. El-Rassy, *Mater. Chem. Phys.*, 2020, **252**, 123296.
61 B. Yang, P. Picchetti, Y. Wang, W. Wang, C. Seeger, K. Bozov, S. Malik, D. Mallach, A. H. Schäfer and M. Ibrahim, *Sci. Rep.*, 2024, **14**, 1249.
62 N. Mizuno and M. Misono, *Chem. Rev.*, 1998, **98**, 199.
63 W. A. Shah, A. Waseem, M. A. Nadeem and P. Kögerler, *Appl. Catal., A*, 2018, **567**, 132.
64 H. Wan, C. Chen, Z. Wu, Y. Que, Y. Feng, W. Wang, L. Wang, G. Guan and X. Liu, *ChemCatChem*, 2015, **7**, 441.

65 M. Simões, C. Conceição, J. Gamelas, P. Domingues, A. Cavaleiro, J. Cavaleiro, A. Ferrer-Correia and R. Johnstone, *J. Mol. Catal. A: Chem.*, 1999, **144**, 461.
66 X.-H. Liu, X.-H. Luo, S.-X. Lu, J.-C. Zhang and W.-L. Cao, *J. Colloid Interface Sci.*, 2007, **307**, 94.
67 R. M. Silverstein and G. C. Bassler, *J. Chem. Educ.*, 1962, **39**, 546.
68 D. L. Pavia, G. M. Lampman, G. S. Kriz and J. R. yvyan, *Introduction to Spectroscopy*, Cengage Learning, 2015.
69 M. Aghayi, B. Yadollahi and M. R. Farsani, *J. Iran. Chem. Soc.*, 2020, **17**, 2895.